Miniature Differential Mobility Spectrometry Using Atmospheric Pressure Photoionization

ARTICLE *in* ANALYTICAL CHEMISTRY · AUGUST 2006

Impact Factor: 5.64 · DOI: 10.1021/ac052213i · Source: PubMed

4 AUTHORS, INCLUDING:

Erkinjon G. Nazarov
Draper Laboratory
93 PUBLICATIONS **2,255** CITATIONS

SEE PROFILE

Anal. Chem. **2006,** *78,* 4553−4563

Miniature Differential Mobility Spectrometry Using Atmospheric Pressure Photoionization

Erkinjon G. Nazarov,*,† Raanan A. Miller,† Gary A. Eiceman,‡ and John A. Stone§

Sionex Corporation, 8-A Preston Court, Bedford, Massachusetts 01730, New Mexico State University, Las Cruces, New Mexico 88003, and Department of Chemistry, Queens University, Kingston, Ontario K7L 3N6, Canada

Positive and negative ion spectra have been obtained with a miniature differential mobility spectrometer equipped with a photoionization source operating at atmospheric pressure. With benzene as a dopant, providing $C_6H_6^+$ as reactant ion, protonated molecular ions and proton-bound dimer ions were obtained with dimethyl methylphosphonate and butanone. The spectra obtained from gas chromatographic injections of aromatic hydrocarbons, benzene, toluene, and the xylenes, produced the molecular ions when the moisture level was very low, but at a high level the hydrated proton was also present. Possible mechanisms for the formation of protonated products are discussed. Negative ions were produced from electron capture by sulfur hexafluoride using benzene or acetone as dopant. Photoionization of nitrogen dioxide led to the formation of the nitrate ion whose yield was a nonlinear function of concentration. The use of a suitable dopant enhanced ion formation by up to 2 orders of magnitude, and limits of detection in both the positive and negative modes were all at the sub ppm_v level. The study makes a strong case for the use of a photoionization source as an alternative to the radioactive ^{63}Ni source.

There is increasing interest in the use of photoionization in analytical mass spectrometry, especially for LC/MS.[1−8] Photoionization with noble gas resonance lamps, including atmosphere pressure photoionization (APPI), is itself not a new technique. However, photoionization is of little value in low-pressure mass spectrometry since there is inefficient ion production and low sensitivity. The introduction of chemical ionization mass spectrometry (CIMS), which operates with an ion source pressure of ~1 mm of Hg, led to a limited number of publications showing the potential of photoionization employing dopants for more efficient photon absorption and the production of reactant ions suitable for analytical purposes. Sieck and co-workers, in a series of papers, laid the groundwork for the understanding of many of the relevant ion−molecule processes, especially those involving hydrocarbons.[9−12] The studies were carried out using different noble gas resonance lamps. Sieck showed that photoionization of cyclohexane, ionization energy (IE) 9.80 eV, in a CI source produced only molecular ions that were effective for the fingerprinting and semiquantitative determination of alkenes and aromatics in fossil fuels.[13] Noble gas resonance lamps have long been standard equipment in gas chromatograph (GC) photoionization detectors operating at atmospheric pressure. Their advantage is that the normal carrier gases, N_2 and He, having ionization energies much higher than the lamp photon energies, provide no ions in competition with dopants and analytes. Commercially available lamps produce resonance photons with upper energies of 10.6 eV (krypton) and 9.8 eV (xenon) so that choice of one or the other provides some selectivity between analytes.

Bruins has shown that APPI is a valid method for liquid chromatography/mass spectrometry, which has the same sample nebulization and vaporization as in atmospheric pressure chemical ionization (APCI) for which ionization is by corona discharge.[14] Several manufacturers now supply APPI sources for LC/MS applications. The authors demonstrated the effective use of dopants, such as acetone (IE = 9.7 eV) and toluene (IE = 8.88 eV), for certain cases when the cross section for photon absorption of the analyte gave insufficient ion intensity. Yang and Henion noted that the LC/MS signal obtained with an APPI detector for idoxifene and its metabolite was dependent on the mobile phase and in particular was suppressed by the presence of water.[3] APPI as applied to LC/MS has recently been reviewed with the stated objective of showing its potential in areas not presently developed and where it may have advantages for molecules not susceptible, or poorly susceptible, to analysis by electrospray or APCI.[2] The

* Corresponding author. E-mail: Egnazarov@sionex.com.
† Sionex Corporation.
‡ New Mexico State University.
§ Queens University.

(1) Wang, G.; Hsieh, Y.; Korfmacher, W. A. *Anal. Chem.* **2005**, *77*, 541−48.
(2) Raffaelli, A.; Saba, A. *Mass Spectrom. Rev.* **2003**, *22*, 318−31.
(3) Yang, C.; Henion, J. *J. Chromatogr., A* **2002**, *970*, 155−65.
(4) Kauppila, T. J.; Kostiainen, R.; Bruins, A. P. *Rapid Commun. Mass Spectrom.* **2004**, *18*, 808−15.
(5) Kauppila, T. J.; Kotiaho, T.; Kostiainen, R.; Bruins, A. P. *J. Am. Soc. Mass Spectrom.* **2004**, *15*, 203−11.
(6) Robb, D. B.; Covey, T. R.; Bruins, A. P. *Adv. Mass Spectrom.* **2001**, *15*, 391−92.
(7) Hanold, K. A.; Fischer, S. M.; Cormia, P. H.; Miller, C. E.; Syage, J. A. *Anal. Chem.* **2004**, *76*, 2842−51.
(8) Rauha, J.; Vuorela, H.; Kostiainen, R. *J. Mass Spectrom.* **2001**, *36*, 1269−80.
(9) Sieck, L. W.; Ausloos, P. *Radiat. Res.* **1972**, *51*, 47−58.
(10) Sieck, L. W.; Ausloos, P. *J. Res. Natl. Bur. Stand., Sect. A* **1972**, *76*, 253−62.
(11) Sieck, L. W.; Lias, S. G.; Hellner, L.; Ausloos, P. *J. Res. Natl. Bur. Stand., Sect. A* **1972**, *76*, 115−24.
(12) Sieck, L. W.; Searles, S. K.; Ausloos P. *J. Res. Natl. Bur. Stand., Sect. A* **1971**, *75*, 147−53.
(13) Sieck, L. W. *Anal. Chem.* **1979**, *51*, 128−32.
(14) Bruins, A. P. In *Electrospray Ionization Mass Spectrometry*; Cole, R. B., Ed.; John Wiley: New York, 1997; p 107.

10.1021/ac052213i CCC: $33.50
Published on Web 05/09/2006

review emphasizes that the mechanisms of formation of some of the ions observed by Bruins and others in APPI are not fully understood. For example, electron transfer from analyte M to a dopant ion, X^+, $M + X^+ \rightarrow M^+ + X$, is not the only reaction observed with toluene; protonated analyte is also observed.

Ion mobility spectrometry (IMS) is a trace analytical technique that can operate at atmospheric pressure when radioactive ^{63}Ni is the usual source of ionizing electrons. This source has high efficiency for many analytes and has the advantage of requiring no power.[15] Both polar and nonpolar analytes can be detected, the efficiency of detection depending on chemical ionization reactions determined by one or more molecular properties, such as ionization potential, proton affinity, electron affinity, etc. For obvious reasons it would be highly advantageous to replace the radioactive source with a photoionization source, and indeed the use of discharge lamps as ionization sources for mobility spectrometers was described early in their development as analytical tools.[16−18] However, development was not pursued. The potential of photoionization as an alternative source for the production of ions in IMS warrants further investigation.

Sionex Inc. has recently developed a differential mobility spectrometer (DMS) that is based on ion separation according to mobility differences in an asymmetric radio frequency electric field. The sensor has high sensitivity and selectivity, low cost, small size, high-speed operation, and the ability to simultaneously provide both positive and negative ion spectra. A number of prototype DMS analytical devices employing either radioactive or a photoionization sources have been developed, and in earlier papers we reported some results obtained with these devices, employing either radioactive or photoionization sources.[19,20] In this paper we describe an extended survey of the capability of photoionization in the instrument, with an investigation of the production of both positive and negative ions, and suggest possible chemical ionization mechanisms for the composition of the ions that appear in the APPI-DMS spectra.

The absorption by a molecule AB of a UV photon with energy $h\nu$ greater than its ionization energy can lead to the formation of a molecular ion and the release of an energetic electron with maximum energy $h\nu$ − IE.

$$AB + h\nu \rightarrow AB^{+}* + e^{-} \quad (1)$$

Absorption of a photon with energy $h\nu$ < IE leads to an electronically excited molecule.

$$AB + h\nu \rightarrow AB* \quad (2)$$

If photon absorption occurs in a gas at atmospheric pressure then the fate of AB^{*+} and AB* will be determined in large part by the gas composition since the collision rate is $\sim 10^{11}$ s^{-1}. The common APPI source is a krypton resonance lamp with maximum photon energy of 10.6 eV, which is usually insufficient to cause dissociative ionization. In most cases $AB^{+}*$ will be thermalized by collision with nonreactive neutral molecules such N_2 and O_2 in air. AB* may suffer the same fate, but there may be sufficient electronic excitation for prompt dissociation to occur. Thermalized AB^+ can participate in competitive ion−molecule reactions at rates determined by rate constants and neutral molecule, M, concentrations. Some common possible reactions are described by eqs 3−5.

$$\text{Electron transfer:} \quad AB^{+} + M \rightarrow AB + M^{+} \quad (3)$$

$$\text{Hydrogen abstraction:} \quad AB^{+} + M \rightarrow ABH^{+} + (M - H) \quad (4)$$

$$\text{Proton transfer:} \quad AB^{+} + M \rightarrow (AB - H) + MH^{+} \quad (5)$$

The energetic photoelectrons are similarly thermalized by collision, when they may be captured either by ions (eq 6) or by molecules with electron affinity (eq 7).

$$e^{-} + AB^{+} \rightarrow AB* \quad (6)$$

$$e^{-} + M \rightarrow M^{-}* \quad (7)$$

The positive and negative product ions may take part in further reactions, including association reactions, with other neutral molecules, for example, proton-bound dimer formation (eq 8) and, for both positive and negative ions, the ubiquitous hydration reactions (eq 9).

$$MH^{+} + M \rightarrow M_2H^{+} \quad (8)$$

$$M^{\pm} + nH_2O \rightarrow M^{\pm}(H_2O)_n \quad (9)$$

In contrast to photoionization under low-pressure conditions, in APPI there can be many routes for transformation of charge from the initially formed ions to those present in the spectra. The types of ions observed in a spectrum will depend on the potential for further ion−molecule reactions, which is determined by the gas composition, the time available for reaction, and the temperature. Therefore, some impurities (or dopants) in the system, including ubiquitous water vapor, may play a crucial role in efficiency and ion species formation.

Experiments were designed to assess the analytical capabilities for trace atmospheric pollutants detection of a miniature APPI-DMS in both the positive and negative ion modes. In the positive ion mode, dimethyl methylphosphonate (DMMP), the commonly used simulant for the nerve gas sarin, and methyl ethyl ketone (MEK) and benzene, common solvents, were studied. The compounds examined in the negative ion mode were sulfur hexafluoride, a potent greenhouse gas used for electrical insulation and for plasma etching in the semiconductor industry, and the nitrogen oxides. Experiments were performed with and without a dopant.

EXPERIMENTAL SECTION

Most of the work described in this paper was performed with a DMS modified to allow both the efficient gas-phase absorption

(15) Eiceman, G. A.; Karpas, Z. *Ion Mobility Spectrometry*; CRC Press: Boca Raton, FL, 1993.
(16) Baim, M. A.; Eatherton, R. L.; Hill, H. H. *Anal. Chem.* **1983**, *55*, 1761−66.
(17) Eiceman, G. A.; Fleischer, M. E.; Leasure, C. S. *Int. J. Environ. Anal. Chem.* **1987**, *28*, 279−96.
(18) Eiceman, G. A.; Vandiver, V. J. *Anal. Chem.* **1986**, *58*, 2331−35.
(19) Eiceman, G. A.; Nazarov, E. G.; Miller, R. A.; Krylov, E. V.; Zapata, A. M. *Analyst* **2000**, *127*, 466−71.
(20) Miller, R. A.; Nazarov, E. G.; Eiceman, G. A.; King, A. T. *Sens. Actuators, A* **2001**, *91*, 301−12.

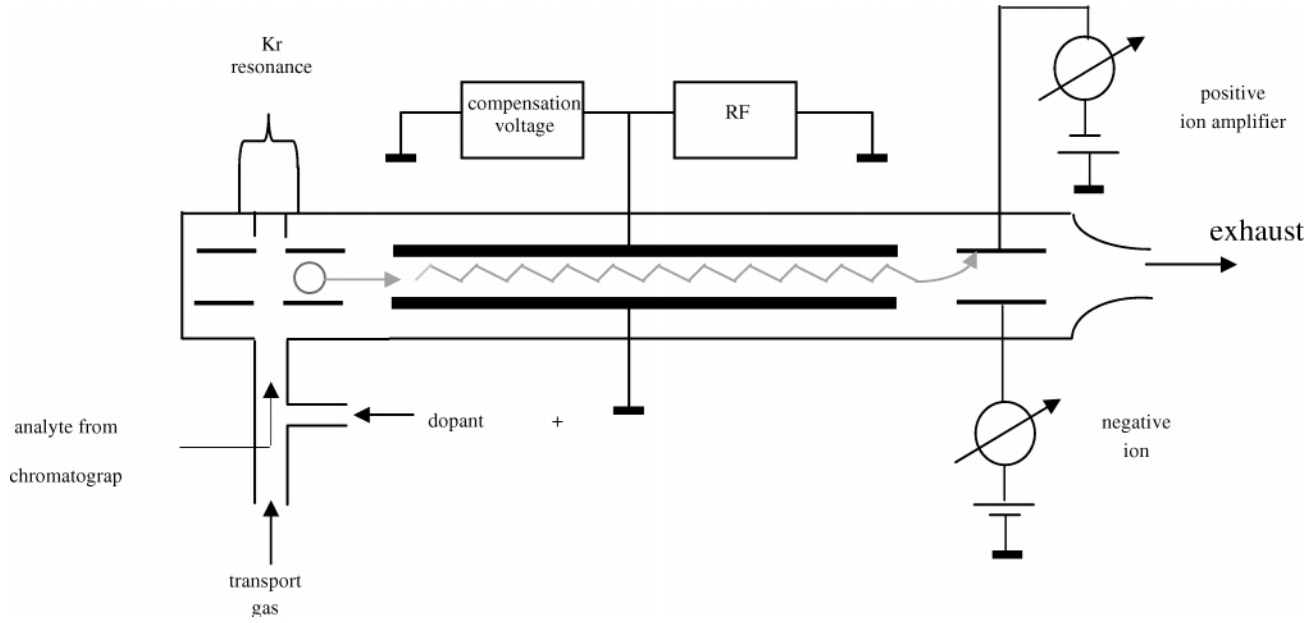

Figure 1. Differential mobility spectrometer (DMS) with a krypton resonance UV lamp as the source of ionization. Analyte can be introduced either via a gas chromatograph or via the port used to introduce dopant.

of photons at atmospheric pressure and the introduction of known analyte concentrations from a gas chromatograph. In a few exponential dilution experiments analyte was introduced directly into the transport gas stream. A sketch of the DMS (model SDP-1, Sionex Inc., Bedford, MA) with the photoionization source is shown in Figure 1. Positive and negative ions formed in the source are carried together by a transport gas between two parallel filter electrodes (separating plates) and are then detected by Faraday plates. The dimensions of the electrodes are as follows: length 15.0 mm; width 3.0 mm; and distance apart 0.50 mm. The volume between the plates is 22.5 mm^3 so that with the usual transport gas flow rate of 1.0 L min^{-1} the residence time of an ion in the analytical section is 1.35 ms.

A miniature krypton discharge lamp with a MgF_2 window (CPI, Santa Rosa, CA) provides photons with energies of 10.6 eV (15−20%) and 10.0 eV (80%). The light is directed down through a tube, i.d. = 4 mm, which supplies the transport gas containing, when required, a known concentration of dopant and 2 cm^3 min^{-1} of helium from a gas chromatograph. To prevent condensation of analyte, the transport gas was preheated so that the DMS temperature was held at 350 K.

The separation of ions formed in the APPI source occurs as they pass in the gas stream through the small gap between the two filter electrodes under the influence of a strong asymmetric waveform 1.18 MHz rf electric field applied perpendicular to the gas flow. The profile of the waveform, shown in Figure 2, has equal integrals above, high field, and below, low field, the zero line. Fields, E_{high} = 30 000 V cm^{-1} and E_{low} = −7200V cm^{-1}, for example, can be generated when the maximum difference between the filter plates, spaced 0.5 mm apart, is +1500 V.

The method and operating principles of the DMS have been described previously in detail.[19−22] The DMS separates ions at

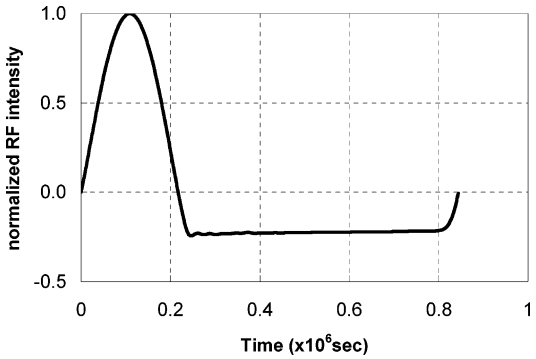

Figure 2. Asymmetric waveform of the DMS electric field. The integrals above and below the 0 line are equal.

ambient pressure (molecule number density N), based on the nonlinear dependence of the mobility coefficient $K(E)$ on the applied electric field (eq 10).[23]

$$K(E) = K(0)[1 + \alpha_2(E/N)^2 + \alpha_4(E/N)^4 + ...] = K(0)[1 + \alpha(E/N)] \quad (10)$$

$K(0)$ is the mobility coefficient for low E conditions, and the α_i parameters show the dependence of K on the electric field, which is specific for each ion.

Nonsymmetric waveform rf impulses applied to the electrodes cause an oscillatory motion of the ions transverse to the flow. This oscillatory motion draws ions toward one electrode or the other with different velocity, $v(t) = K(E)E(t)$, in each portion of the waveform. Ions can pass through the narrow channel between the electrodes and subsequently be detected only if the net displacement caused by the high- and low-voltage portions of the nonsymmetric rf pulses is close to zero. If an ion has some net lateral displacement, i.e., different α parameters for the high- and

(21) Buryakov, I. A.; Krylov, E. V.; Nazarov, E. G.; Rasulev, U. K. *Int. J. Mass Spectrom. Ion Processes* **1993**, *128*, 143−48.
(22) Purves, R. W.; Guevremont, R.; Day, S.; Pipich, C. W.; Matyjaszczyk, M. S. *Rev. Sci. Instum.* **1998**, *69*, 4094−105.
(23) Mason, E. A.; McDaniel, E. W. *Transport Properties of Ions in Gases*; John Wiley: New York, 1988.

low-field periods, after a certain time it will collide with one of the electrodes and not pass through the filter.

The lateral displacement of any ion species through the analytical gap can be adjusted to zero by imposing a dc potential V_c, the compensation voltage, on one of the electrodes that compensates for the effect of the rf. V_c is scanned to record a DMS spectrum. Both positive and negative ions are carried together through the analytical gap by the transport gas and can therefore be detected concurrently as V_c is scanned. The detector ion current, as a function of V_c, provides spectral information characteristic of ions having different α values. Since the dependence of α on the rf amplitude is nonlinear, the amplitude is an additional variable that may also be scanned to provide additional information.

A few experiments were carried out with an APPI-DMS coupled to a mass spectrometer in the manner previously described.[24] In this DMS one of the detector plates is used as a deflector plate to direct ions toward the opposite plate that has an orifice leading to the mass spectrometer. The design of this APPI-DMS/MS system however has a major flaw. For example, a protonated molecule MH^+ will be in equilibrium with a proton-bound dimer M_2H^+ and M in the source region. When MH^+ traverses the analytical gap at the appropriate V_c, the M_2H^+, having a different V_c, has been eliminated by discharge at an electrode. In the brief time spent in the detection region prior to entering the mass spectrometer, MH^+ has the opportunity to form some M_2H^+ by associating with M present in the transport gas. The mass spectrum then shows not only the separated ion but other ions formed postseparation. Because of this effect and also because of low ion intensity, mass spectra were obtained with no separating rf field or compensation voltage; the spectra then show all the ions resulting from the initial photoionization.

A clean air generator (model 737, Addco Corp, Miami, FL) was used to provide the gas flow to the DMS. In a few experiments bottled nitrogen was used. The gas was scrubbed through beds of activated charcoal and 13X molecular sieve to provide a moisture level in the range of 0.5−1 ppm_v. The purified gas was split into three independently controlled streams: up to 1.00 L min^{-1} for transport gas; when required, 10−300 cm^3 min^{-1} to operate a diffusion-based vapor generator providing analyte or dopant that was further diluted by a 0−300 cm^3 min^{-1} stream to obtain an appropriate concentration. All supply lines after the vapor generator were kept at ∼60 °C to minimize wall adsorption. By adjusting the ratio of analyte to dilution flows and the flow of transport gas, the system allowed a constant gas flow of 1.00 L min^{-1} to be delivered to the DMS, while permitting changes in vapor concentration. Total flow was monitored at the DMS exhaust.

All the chemicals, acetone, benzene, toluene, xylenes, dimethyl methylphosphonate, and butanone were obtained from the Aldrich Chemical Co. (St. Louis, MO) and were used without further purification. Gaseous analytes, toluene in N_2 (1−10 ppm), sulfur hexafluoride (10 ppm) in N_2, NO, and NO_2 were obtained from Scott Specialty Gases (Plumsteadville, PA).

RESULTS AND DISCUSSION

Positive Ion Spectra. Prior to installation in the DMS, experiments were carried out with the krypton lamp to determine the extent of photon beam attenuation with distance. The light intensity, attenuated by scattering and absorption in air, was measured as a function of distance x (mm) from the MgF_2 window and was found to decay exponentially according to the equation $\ln(I/I_0) = -0.46x$. The beam therefore loses 50% of its intensity every 1.5 mm. Ion formation occurred not only in the 0.5 mm gap but also in the 4 mm diameter inlet pipe (see Figure 1), ensuring efficient ion production. In the absence of an rf field, ions produced by photoionization were carried by the transport gas to the detector with no separation. Since all the main components of the purified air, nitrogen, oxygen, argon, carbon dioxide, and water, have ionization energies higher than the maximum photon energy of the krypton lamp, no ions were produced when only the transport gas was present. The DMS spectrum showed a flat baseline in both positive and negative modes. The introduction of 2 ppm_v of benzene (IE = 9.24 V) into the transport gas in the absence of an rf field gave, as expected, a single DMS peak at V_c very close to 0 V. As was found in previous work,[19] peak intensities and compensation voltages obtained under the same experimental conditions were reproducible to within ±6%. The benzene molecular ion was the only ion produced (eq 11); the isomeric fulvene ion, although having a lower ionization energy (8.36 eV), cannot be formed since the isomerization barrier is 1.6 eV[25] and there are no possible fragment ions below 13 eV.

$$C_6H_6 + h\nu \rightarrow C_6H_6^+ + e^- \qquad (11)$$

When the rf field was applied, the value of V_c at which the peak appeared became negative, the value increasing with increasing amplitude as seen in Figure 3a.

The signal intensity at peak maximum initially increased slightly as the amplitude increased but then declined as graphed in Figure 3b. This slight increase, which was reproducible, does not indicate an increase in the total number of ions reaching the detector but rather a slight narrowing of the peak, since the number of ions, determined by peak area, decreases monotonically with increasing rf amplitude. The values of V_c at the peak maxima are shown in Figure 3c. For analytical purposes an rf amplitude must be chosen such that there is sufficient peak intensity with good resolution. The instrument was usually operated with an amplitude of +1000 V, giving a maximum high field of 2.00×10^4 V cm^{-1}.

DMMP. The usefulness of benzene as a dopant in the positive ion mode is illustrated in Figure 4 for experiments in which DMMP (IE = 10.0 eV) was introduced via the chromatograph. Each of the three pairs of curves in the figure shows the positive ion DMS spectrum obtained in the absence (upper dotted spectrum) and presence (lower solid spectrum) of DMMP. These DMS spectra, and all others obtained after a chromatographic injection, correspond to the spectra obtained at the maximum of analyte concentration. In the presence of dopant, this occurs at

(24) Eiceman, G. A.; Nazarov, E. G.; Miller, R. A. *Int. J. Ion Mobility Spectrom.* **2000**, *3*, 15−27.

(25) Rusyniak, M.; Ibrahim, Y.; Alsharaeh, E.; Meot-Ner, M.; El-Shall, S. M. *J. Phys. Chem. A* **2003**, *107*, 7656−66.

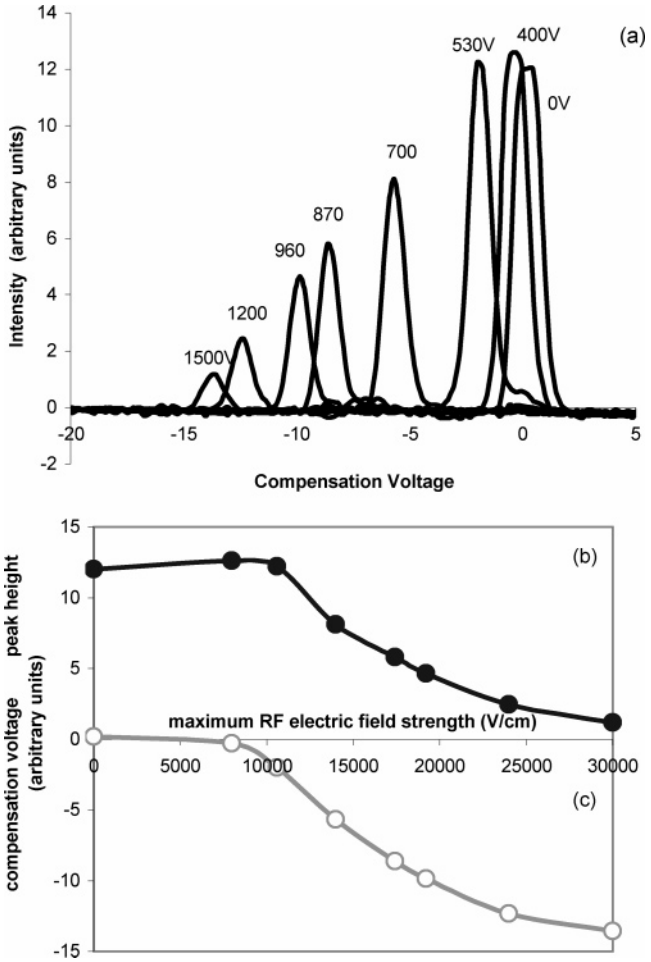

Figure 3. Effect of maximum rf field, from 0 to 30 000 V cm^{-1}, on the benzene (2 ppm_v) DMS positive ion spectrum. (a) Spectra at different field strengths; (b) peak height; (c) compensation voltage at peak position.

the time of minimum dopant ion signal. In the absence of dopant, it is the time of maximum signal intensity.

No ions were formed from air alone, as shown by the horizontal dotted line of spectra 1. A chromatographic injection of 2.24×10^{-6} g DMMP, estimated to yield a concentration of ~0.40 ppm_v in the transport gas at peak maximum, produced a very weak, but reproducible, signal at $V_c = +0.7$ V (solid spectrum 1). A concentration of 2.0 ppm_v of benzene alone in the transport gas produced a large signal at $V_c = -10.0$ V (dotted spectra 2 and 3). The cross section of DMMP for photoionization by the krypton resonance radiation is obviously much smaller than that of benzene. With benzene present at 2.0 ppm_v and a DMMP injection of 5.5×10^{-8} g (~10 ppb_v at peak maximum), the benzene peak decreased by about a factor of 2 from the value in the absence of DMMP (solid spectrum 2). Two new peaks appeared, at $V_c = -6.4$ and +0.7 V, the latter being the smaller of the two. When the amount of DMMP was increased to 3.3×10^{-7} g (~60 ppb_v), the benzene peak almost completely disappeared and the +0.7 V peak was dominant (solid spectrum 3).

The DMMP peaks at −6.4 and +0.7 V are, respectively, the protonated molecule, $(DMMP)H^+$, and the proton-bound dimer $(DMMP)_2H^+$. These assignments are based on previous DMS/MS experiments. DMMP, having the higher ionization energy, cannot donate an electron to the benzene cation to produce

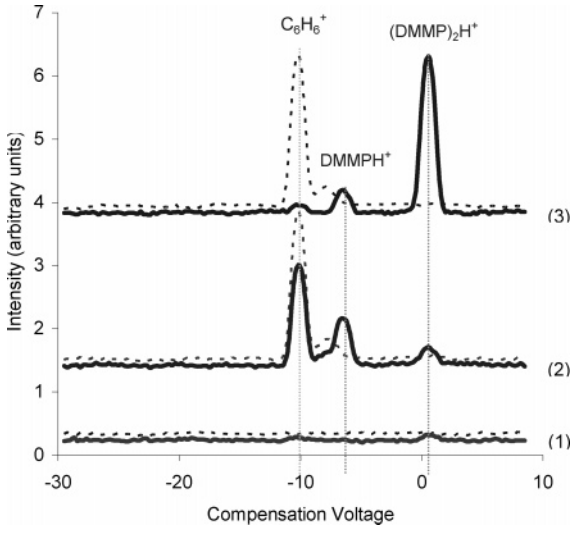

Figure 4. DMS positive ion spectrum of DMMP: (1) 4.0×10^2 ppb_v with no dopant; (2) 10 ppb_v with 2 ppm_v benzene dopant; (3) 60 ppb_v with 2 ppm_v benzene dopant. The upper graph (dotted plot) of each pair, which is displaced upward for easier visualization, shows the appropriate spectrum in the absence of DMMP.

$DMMP^+$. However, the origin of the $(DMMP)H^+$ may be direct proton transfer from $C_6H_6^+$ (eq 12). With data from ref 26 and a proton affinity for DMMP of 902 kJ mol^{-1},[27] the standard enthalpy change for eq 12, ΔH_{12}^0, is −18.8 kJ mol^{-1}. An exothermicity of this magnitude usually ensures that a proton-transfer reaction will proceed with high efficiency.[28] Proton-bound dimer formation by association with another DMMP molecule follows with high efficiency at ambient pressure (eq 13).

$$C_6H_6^+ + DMMP = C_6H_5 + (DMMP)H^+ \qquad (12)$$

$$(DMMP)H^+ + DMMP \rightarrow (DMMP)_2H^+ \qquad (13)$$

With chromatographic injection and the fast scanning time of the DMS (≤ 1.0 s/scan) it is possible to examine the evolution of the monomer and dimer peaks over the GC peak profile. Figure 5 shows the signals obtained from the chromatographic injection of DMMP, the transport gas being air containing 3 ppm_v of benzene. Graph 1 shows the decrease in the benzene signal that, when inverted, is the concentration profile of the analyte eluting from the chromatograph.

This decrease is accompanied by the appearance of both $(DMMP)H^+$ and $(DMMP)_2H^+$ with very different profiles. The $(DMMP)H^+$ intensity, graph 2, rises very sharply and decreases almost immediately as the increasing DMMP concentration favors $(DMMP)_2H^+$ formation (graph 3). The maximum concentration of DMMP is signaled by the $(DMMP)_2H^+$ peak maximum when $(DMMP)H^+$ has almost zero intensity. As the DMMP concentration decreases the $(DMMP)_2H^+$ intensity decreases, and the $(DMMP)H^+$ intensity increases again and finally decays away.

(26) Linstrom, P. J.; Mallard, W. G., Eds. *National Institute of Standards and Technology Standard Reference Database*; No. 69; National Institute of Standards and Technology: Gaithersburg, MD, 2003.
(27) Tabrizchi, M.; Shooshtari, S. *J. Chem. Thermodyn.* **2003**, *35*, 863−70.
(28) Hemsworth, R. S.; Payzant, J. D.; Schiff, H. I.; Bohme, D. K. *Chem. Phys. Lett.* **1974**, *26*, 417−21.

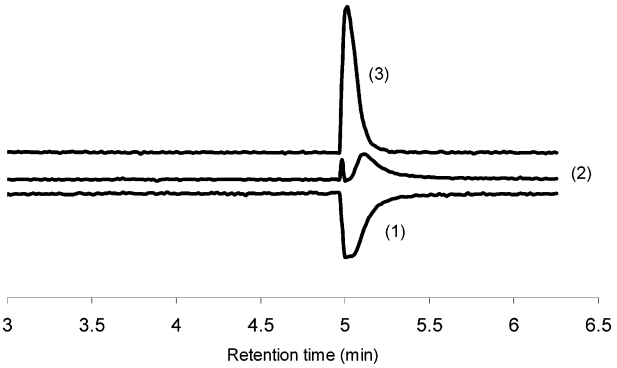

Figure 5. Evolution of the positive ion DMS peaks, as functions of chromatographic retention time, obtained with 3 ppm_v benzene as dopant and a 1.6 ng injection of DMMP: (1) decrease in $C_6H_6^+$ peak intensity; (2) $(DMMP)H^+$; (3) $(DMMP)_2H^+$.

Table 1. Limits of Detection (ppb_v) at a Signal-to-Noise Ratio of 3:1

	ionization method		
analyte (mode)	APPI (no dopant)	APPI (dopant)	^{63}Ni[a]
DMMP (+)	2×10^3	5.2 (acetone) 0.7 (benzene)	1.0
benzene (+)	3×10^2		
butanone (+)	55	1.7 (benzene)	
nitric oxide (+)	3×10^2		
nitrogen dioxide (−)	1×10^3		
sulfur hexafluoride (−)		1×10^2 (acetone) 1×10^2 (toluene)	0.2

[a] Unpublished result from this laboratory.

The appearance of a small signal at $V_c = +0.7$ V, obtained with the high concentration of DMMP in the absence of benzene, requires an explanation since this is the same V_c for $(DMMP)_2H^+$. The molecular cation of DMMP is known to spontaneously isomerize to the enol form,[29,30] yielding a cation with an acidic proton that can be transferred to another DMMP forming $(DMMP)H^+$. Because DMMP has a low photoionization cross section, a high concentration is required to observe a visible signal, and at this high concentration essentially all the $(DMMP)H^+$ reacts to form the observed $(DMMP)_2H^+$.

The estimated limits of detection for DMMP, shown in Table 1, at a 3:1 signal-to-noise ratio was 2 ppm_v with no dopant and 0.7 ppb_v with benzene as dopant. With acetone as dopant the limit of detection was 5.2 ppb_v. For comparison, experiments using ^{63}Ni ionization gave essentially the same limit of detection, 1.0 ppb_v.

Butanone. Butanone, with an ionization energy of IE = 9.52 eV, cannot transfer an electron to $C_6H_6^+$ ($IE(C_6H_6) = 9.23$ eV) and, from its proton affinity of 827 kJ mol^{-1}, the reaction of eq 14 is endothermic by 67.4 kJ mol^{-1} and cannot occur to a measurable extent.

$$C_6H_6^+ + C_4H_8O \rightarrow C_6H_5 + C_4H_8OH^+ \qquad (14)$$

However, protonated butanone is the product observed, confirmed by mass spectrometry, when benzene is used as dopant.

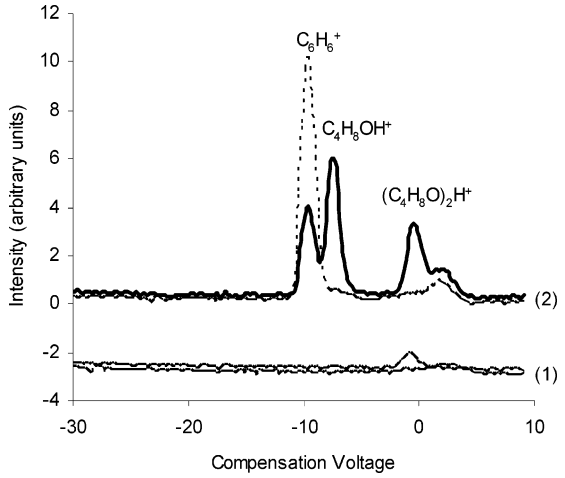

Figure 6. DMS positive ion spectrum spectra obtained with a chromatographic injection of butanone: (1) 12 ng with no dopant; (2) 0.12 ng with 2 ppm_v benzene dopant. The upper graph (dotted plot) of each pair shows the spectrum in the absence of butanone.

The results obtained when butanone was introduced via the chromatograph in the absence and presence of benzene as dopant are shown in Figure 6. A very small signal at $V_c = -0.5$ V was obtained with a 12 ng injection (~29 ppb_v maximum concentration in the transport gas) of butanone in the absence of benzene. With 2 ppm_v of benzene as dopant and a 0.12 ng injection of butanone, a large signal at −7.6 V, protonated butanone, and a smaller one at −0.5, the proton-bound dimer, were observed, while the benzene peak was reduced in intensity by approximately a factor of 3.

There are several possibilities for the formation of protonated analytes by photoionization using an aromatic as the dopant for which the reaction of eq 14 is not possible. For example, a reaction of the initially produced benzene or toluene molecular ions with oxygen (eq 15) has been shown to produce the molecular ion of phenol.[31]

$$C_6H_6^+ + O_2 \rightarrow C_6H_5OH^+ + O \qquad (15)$$

The phenol molecular ion then donates a proton to a suitable analyte, for example, butanone (eq 16).

$$C_6H_5OH^+ + C_4H_8O \rightarrow C_6H_5O + C_4H_8OH^+ \qquad (16)$$

Reaction 15 is almost thermoneutral (−2.4 kJ mol^{-1}), while reaction 16 is endothermic by 33.6 kJ mol^{-1} and is therefore likely to have a very low reaction rate. An earlier study of the photoionization of toluene with mass spectral identification of products found that, in addition to the molecular ion, a peak at m/z 106 constituted about 5% of total ionization.[24] This ion could be the O adduct of the toluene molecular ion or the molecular ion of a xylene impurity. In either case the ion constituted a very low proportion of total ionization, as was found previously for low

(29) Holtzclaw, J. R.; Wyatt, J. R. *Int. J. Mass Spectrom. Ion Processes* **1998**, *23*, 261−6.

(30) Zeller, L.; Farrell, J.; Kenttamaa, H. I.; Vainiotalo, P. *J. Am. Chem. Soc.* **1992**, *114*, 1205−14.

(31) Tubaro, M.; Marotta, E.; Seraglia, R.; Traldi, P. *Rapid Commun. Mass Spectrom.* **2003**, *17*, 2423−29.

concentrations of both benzene and toluene.[31] Since Figure 6 shows that the benzene molecular ion is severely depleted in the presence of only 0.29 ppb_v of butanone, protonation via eqs 15 and 16 is highly unlikely.

A second possibility is proton transfer to butanone from a hydrated proton formed by the reaction of the benzene cation with water vapor.

$$C_6H_6^+ + nH_2O \rightarrow C_6H_6^+(H_2O)_n \quad (17)$$

$$C_6H_6^+(H_2O)_n \rightarrow C_6H_5 + (H_2O)_nH^+ \quad (18)$$

$$(H_2O)_nH^+ + C_4H_8O \rightarrow C_4H_8OH^+ + nH_2O \quad (19)$$

The formation of the hydrated proton by this mechanism is well documented.[32−35] The thermodynamics of the stepwise hydration of the benzene cation has been studied using a mass-selected drift tube operating with about 0.2 torr of water vapor.[35] The standard enthalpy and entropy changes for association with the first two water molecules are, respectively, −38 kJ mol^{-1} and −82 J K^{-1} mol^{-1} and −33 kJ mol^{-1} and −79 J K^{-1} mol^{-1}. The enthalpy change for the addition of the first water molecule is in fair agreement with the 59 ± 13 kJ mol^{-1} binding energy estimated from frequency shifts.[32] The calculated relative equilibrium concentrations of the benzene cation and its monohydrate at 350 K in the presence of 1 ppm_v of water using the above data is $1:2 \times 10^{-5}$; higher hydrates have negligible relative concentrations. Since the reaction of eq 18 does not occur for $n \leq 3$,[33−35] the formation of a protonated species via the hydrated proton derived from the hydrated benzene cation is improbable under our experimental conditions of low water concentration.

A third possibility has butanone forming a complex with the benzene cation and a second butanone subsequently aiding in deprotonation (eqs 20, 21).

$$C_6H_6^+ + C_4H_8O \rightarrow C_6H_6^+(C_4H_8O) \quad (20)$$

$$C_6H_6^+(C_4H_8O) + C_4H_8O \rightarrow [C_6H_6^+(C_4H_8O)_2]^* \rightarrow C_6H_5 + (C_4H_8O)_2H^+ \quad (21)$$

Because of its much higher proton affinity (827 kJ mol^{-1}) than that of water (691 kJ mol^{-1}) butanone will solvate the benzene cation more strongly than does water. The enthalpy change for the combination of reactions 22 and 23 is −60 kJ mol^{-1}, so the protonation scheme is feasible. For this scheme to be possible under the experimental conditions, the lifetime of $C_6H_6^+(C_4H_8O)$ must be sufficiently long that reaction 21 can occur. $(C_4H_8O)H^+$ would then also be formed as $(C_4H_8O)_2H^+$ tends toward equilibrium with neutral butanone.

An alternative to reaction 21 involves a water molecule, instead of the second butanone molecule, effecting the deprotonation (eq 22).

$$C_6H_6^+(C_4H_8O) + H_2O \rightarrow [C_6H_6^+(C_4H_8O)(H_2O)]^* \rightarrow C_6H_5 + H^+(C_4H_8O)(H_2O) \quad (22)$$

Although the enthalpy change for this exothermic reaction is only −8 kJ mol^{-1}, the much higher concentration of water than of butanone could favor it over the competing mechanism. This third possibility (eqs 20 and 21 and/or 20 and 22) appears to be the most favorable for protonated analyte formation, not only for butanone, but maybe also for DMMP and other molecules. The formation of the hydrated proton was observable when aromatic hydrocarbons were photoionized in the presence of high concentrations of water. Figure 7 shows two-dimensional contour plots of DMS signal versus time as ∼10 ng of each of benzene, toluene, ethyl benzene, and *o*-, *m*-, and *p*-xylene eluted from the chromatograph into the gas stream containing (a) 1 ppm_v and (b) 1.3×10^3 ppm_v of water vapor. In Figure 7a, peaks due to the individual aromatic cations appear at less negative V_c values as the molar mass increases. This trend of increasing V_c with increasing ion mass has been noted previously for a homologous series of ketones.[36] The presence of a high water vapor concentration resulted in a lower total signal intensity and the appearance with each cation signal of a new peak at the same V_c, = −18.68 V (Figure 7b). This new signal is due to the hydrated proton, consistent with the high degree of hydration of the benzene cation required for its formation.[32−35]

With the thermodynamic data from ref 35, the calculated relative concentrations of the bare, the mono-, the di-, and the trihydrate of the benzene cation at 350 K for 1 ppm_v of water vapor are $1:2 \times 10^{-5}:2 \times 10^{-10}:7 \times 10^{-16}$ and for 1300 ppm_v are $1:3 \times 10^{-2}:3 \times 10^{-4}:2 \times 10^{-6}$. Even with the higher concentration of water vapor the equilibrium concentration of the trihydrate is very small so that its reaction to form the hydrated proton must occur with high efficiency. It is notable that the signal for the hydrated proton is greatest and the associated signal for the aromatic cation is least for ethylbenzene. This is the only molecule with a methylene group, for which the exothermicity of deprotonation is less than that for the methyl groups present in the other molecules.

The hydrated proton signal in Figure 7b had the peculiarity that it was always delayed by the time of one scan, 1.00 s, from the aromatic cation signal. This is shown in Figure 7c for the sequential scans at chromatographic retention times of 46.5 and 47.5 s, the former dominated by the benzene cation peak and the latter by the hydrated proton peak. Considering that the residence time of an ion or molecule in the instrument, determined by the transport gas flow rate, was considerably less than 1 s, the explanation for the phenomenon is not immediately obvious. The possibility of a surface-induced reaction cannot be eliminated.

NO_x. NO and NO_2 but not N_2O were examined. The latter has an ionization energy of 12.90 eV and an electron affinity that is no greater than 0.22 eV, and may even be negative,[37] rendering it unavailable for analysis by photoionization or electron capture in the present instrument.

(32) Solca, N.; Dopfer, O. *Chem. Phys. Lett.* **2001**, *347*, 59−64.
(33) Miyazaki, M.; Fujii, A.; Mikami, N. *J. Phys. Chem. A* **2004**, *108*, 8269−72.
(34) Miyazaki, M.; Fujii, A.; Ebata, T.; Mikami, N. *Chem. Phys. Lett.* **2004**, *399*, 412−16.
(35) Ibrahim, Y.; Alsharaeh, E.; Dias, K.; Meot-Ner, M.; El-Shall, M. S. *J. Am. Chem. Soc.* **2004**, *126*, 12766−67.
(36) Krylov, E.; Nazarov, E. G.; Miller, R. A.; Tadjikov, B.; Eiceman, G. A. *J. Phys. Chem. A* **2002**, *106*, 5437−44.
(37) McCarthy, M. C.; Allington, J. W. R.; Sullivan, K. O. *Mol. Phys.* **1999**, *96*, 1735−37.

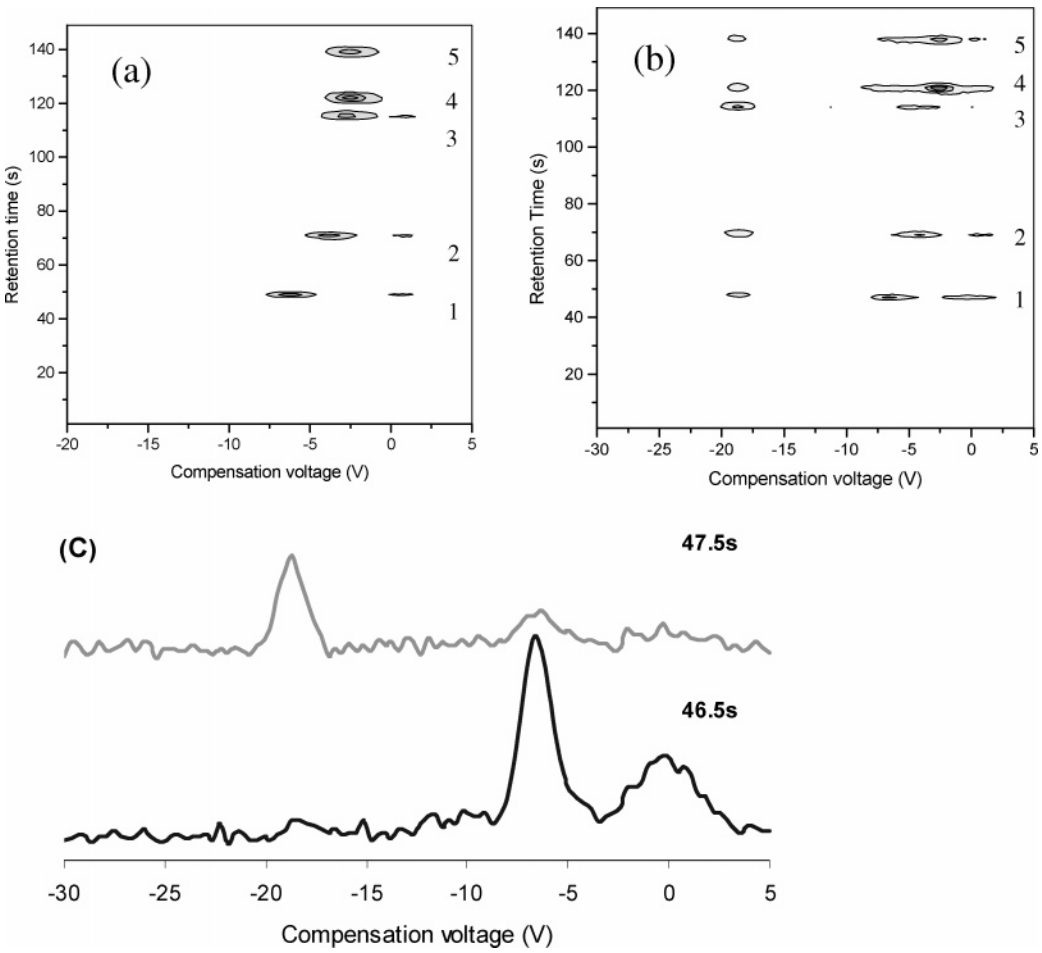

Figure 7. Contour plots showing peak intensity in the DMS spectrum for a series of aromatic hydrocarbons eluted from the chromatograph. Transport gas containing (a) ~1 ppm_v water vapor and (b) 1.3×10^3 ppm_v water vapor. Injection: 10 ng of each of 1, benzene; 2, toluene; 3, ethylbenzene; 4, *m*- and *p*-xylene; and 5, *o*-xylene. (c) DMS spectra obtained 1 s apart in the presence of 1.3×10^3 ppm_v water vapor, with benzene at $V_c = -7$ V, elutes at a retention time of 46.5 s.

NO has an ionization energy of 9.26 eV, which is almost identical with that of benzene, and therefore the use of an aromatic as dopant in its analysis was not possible. An extremely low proton affinity of 532 kJ mol^{-1} also negates protonation as a possible ionization mechanism. The DMS spectrum of NO showed a single peak at −23.6 eV, due to NO^+. Both the peak area and peak height of the signal are linear with NO concentration up to 5 ppm_v as shown in Figure 8. At higher concentration the signal has a constant value. The limit of detection by direct photoionization for a signal-to-noise ratio of 3:1 was determined as 3×10^2 ppb_v (Table 1).

NO_2 with an ionization energy of 9.589 eV is directly ionizable by the krypton radiation. Two DMS peaks were produced, the smaller of the two at $V_c = -23.6$ V corresponded in position to that of NO^+ while that at −17.8 V was presumably due to NO_2^+. NO^+ cannot arise from direct photoionization since the appearance energy of NO^+ from NO_2 is12.34 eV. However, at 10 eV, photolysis of NO_2 to NO and O is possible.[38] This reaction may be the source of neutral NO, which then forms NO^+ by electron transfer to NO_2^+. The limit of detection for NO_2 was determined as 1×10^3 ppb_v.

(38) Lahmani, F.; Lardeux, C.; Solgadi, D. *J. Chim. Phys. Phys.-Chim. Biol.* **1983**, *80*, 705−09.

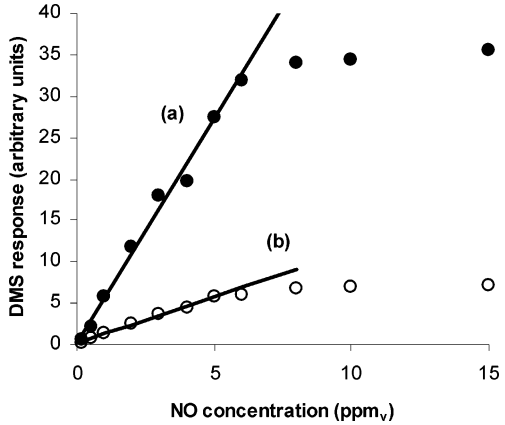

Figure 8. Positive ion DMS signal as a function of NO concentration: (a) peak area, $A = 5.4285c + 0.329$, $R^2 = 0.9864$; (b) peak height, $H = 1.1202c + 0.1404$, $R^2 = 0.9946$.

Negative Ions. The electrons produced in the photoionization of a molecule have low initial energies. The maximum value of the energy is the difference between the photon energy and the ionization energy of the absorbing molecule. For benzene, for example, the value would be 10.6 eV − 9.2 eV = 1.4 eV. An electron with such an initial energy has a short path length in the field-free region of the source before becoming thermalized

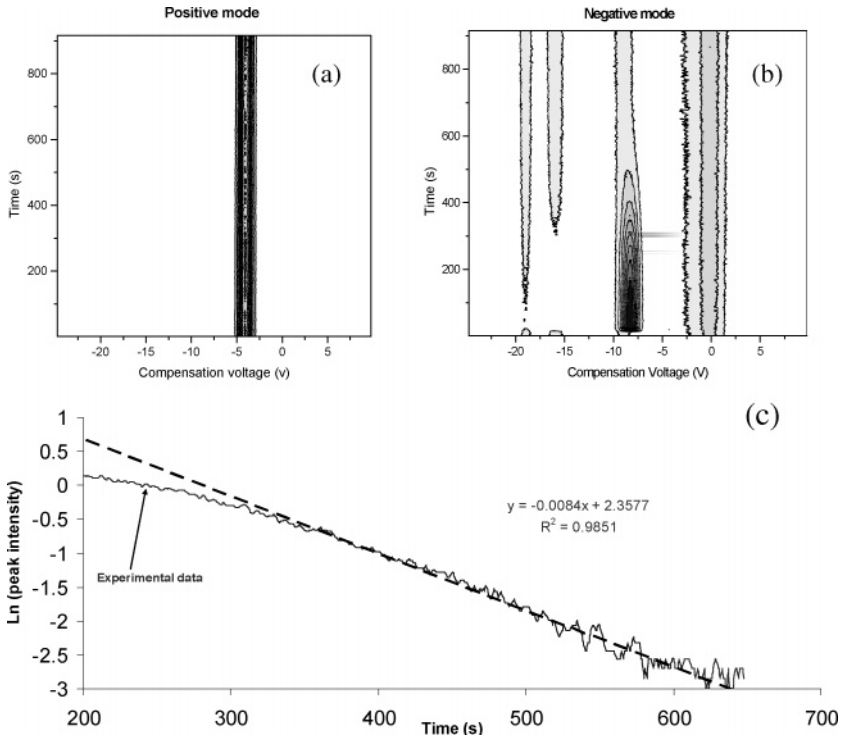

Figure 9. Exponential dilution experiment with SF_6. (a) DMS positive ion spectrum; the single signal is due to acetone dopant. (b) DMS negative ion spectrum. SF_6^- appears at a compensation voltage of ~ -8 V. The negative ions at $V_c = 0$ V are unaffected by the presence of SF_6, while those at $V_c = -16$ and -19 V are eliminated at high concentration and reappear as the concentration declines. (c) The exponential decay of the SF_6^- peak height as a function of time.

by collision with the transport gas and would be unlikely to be lost to the walls. The reservoir of electrons for reaction by electron capture should therefore be as great as that for the positive ions. Molecules with low ionization energies and positive electron affinities may produce their own negative ions after photoionization. Molecules with ionization energies greater than the maximum photon energy require a suitable dopant to provide the electrons. A dopant is preferable in most cases since, if there is a very low concentration of analyte and it is the only source of electrons, few electrons will be produced and the second-order electron capture reaction will be highly inefficient. The production of negative ions from sulfur hexafluoride, NO_2, and NO was investigated.

Sulfur Hexafluoride. The reaction of SF_6 with thermal electrons proceeds at essentially the maximum (Langevin) rate with $k = 2.3 \times 10^{-7}$ cm^3 molecule^{-1} s^{-1}, independent of temperature.[39] SF_6 has an electron affinity of 1.070 ± 0.070 eV,[26] and SF_6^- is very stable toward thermal electron detachment, $SF_6^- \rightarrow SF_6 + e^-$. The maximum E/N value in the present work was 125 Td (1 Td = 10^{-17} V cm^2), and there is no evidence for the thermal detachment of electrons for E/N values up to 400 Td and temperatures up to 600 K.[40] The dissociation of nascent SF_6^- (containing excitation energy due to electron attachment) under ambient conditions is of low probability since the second excited state leading to $SF_5^- + F$, which at its potential minimum has the same geometry as the SF_6^- ground state, is easily collisionally quenched. The $[SF_5^-]/[SF_6^-]$ ratio is found to be less than one part in 10^5 at temperatures below 500 K.[41] The above suggests that if thermalized electrons are produced in air they may be captured by SF_6 at every collision to produce SF_6^- at a rate independent of temperature, and these ions should be stable toward electron detachment, even in the DMS rf field. The origin of the anion will depend on the concentration of SF_6 since there is competition for electrons with components, mainly oxygen, of the transport gas. At high concentration, direct electron capture by SF_6 can occur, but at trace levels electron transfer from anions of lower electron affinity than SF_6 will be prevalent.

SF_6 has an ionization energy of 15.32 eV, and so negative ions can be formed only by use of a dopant. With no SF_6 or dopant present there was no photon absorption, and hence, neither a positive ion signal nor a negative ion signal was observed. The lack of a negative ion signal showed that electrons were not being produced by photoelectron emission from a surface in the vicinity of the krypton lamp as was found by Basso et al. in their APPI study of the formation of negative ions.[42] Figure 9 shows contour plots of V_c versus time for both positive (Figure 9a) and negative (Figure 9b) ions in an exponential dilution experiment with acetone as dopant and an initial SF_6 concentration of 500 ppm$_v$.

Acetone has an ionization energy of 9.70 eV and gave one peak of constant intensity in the positive mode, at $V_c = -4.9$ V. It has no electron affinity, but in the absence of SF_6, unidentified negative ions were present in the spectra at -19, -16, and 0 V. Figure 9b shows that the introduction of $\sim 5 \times 10^2$ ppm$_v$ of SF_6 in a dilution experiment generated a very large signal at $V_c \sim -8.0$ V. The

(39) Hunter, S. R.; Carter, J. G.; Christophorou, L. G. *J. Chem. Phys.* **1989**, *90*, 4879–91.
(40) Datskos, P. G.; Christophorou, L. G.; Carter, J. G. *J. Chem. Phys.* **1993**, *99*, 8607–16.
(41) Chen, E. C. M.; Shuie, L. R.; D'sa, E. D.; Batten, C. F.; Wentworth, W. E. *J. Chem. Phys.* **1988**, *88*, 4711–19.
(42) Basso, E.; Marotta, E.; Seraglia, R.; Tubaro, M.; Traldi, P. *J. Mass Spectrom.* **2003**, *10*, 1113–15.

appearance of this signal was accompanied by the disappearance of the signals at −19 and −16 V. These signals must be due to ions, such as O_2^- and O_4^-, formed from species having lower electron affinities than SF_6. The 0 V signal was not affected, the associated molecule presumably having a higher electron affinity than SF_6. As the SF_6^- signal decreased in intensity with decreasing SF_6 concentration, first the −19 V signal and then the −16 V signal reappeared. The decay of the SF_6^- signal as a function of time is shown in Figure 9c.

There is initial detector saturation followed by an exponential decay at low concentration after ~350 s that extends over a concentration range of only 1 order of magnitude. A series of experiments determined a limit of detection for SF_6 of 1×10^2 ppb_v, defined with a signal-to-noise ratio of 3:1. Acetone was the dopant in this experiment, but an aromatic such as toluene was equally effective in supplying the required electrons and yielded the same negative ion spectra and limit of detection.

Table 1 shows that the limit of detection for SF_6, obtained by photoionization with a dopant, is 50 times greater than that obtained with ^{63}Ni ionization, for which of course a dopant is not necessary to provide an ample supply of thermalized electrons. This is somewhat surprising since the limit of detection for DMMP in the positive ion mode with the same dopant is the same as that obtained with ^{63}Ni ionization.

NO and NO_2. Although the photoionization of NO produces electrons, no negative ions attributable to NO were found in its DMS spectrum over the concentration range of 0−15 ppm_v. The molecule has an electron affinity of 0.026 eV and so cannot compete for electrons with other molecules present in the system, including oxygen, that have substantially higher electron affinities. In contrast to NO, NO_2 with an electron affinity of 2.27 eV shows a single large negative ion peak, at $V_c = -10$ V.

The mass spectrum of the NO_2 system in the negative ion mode was simple in dry nitrogen, containing ions at m/z 62, 125, and 188. When the nitrogen was humidified, the intensities of all these ions were reduced as m/z 188 was hydrated by up to seven water molecules. The ion at m/z 62 was presumed to be NO_3^-, and m/z 125 and 188 were then NO_3^- solvated by, respectively, one and two HNO_3 molecules. Figure 10 shows that the DMS signal, whether measured as peak height or peak area, has a nonlinear dependence on the NO_2 concentration. The equations, $A = 0.0555c^2 + 1.643c - 1.9066$ and $H = 0.0042c^2 + 0.2764c - 0.2651$, fit the lines describing peak area A and peak height H, in arbitrary units, where c is the NO_2 concentration in ppm_v.

At low concentration, electron capture by oxygen will take precedence over electron capture by NO_2. Exothermic O^- transfer to NO_2 (eq 23) then leads to the formation of NO_3^-.

$$NO_2 + O_2^- \rightarrow NO_3^- + O \qquad \Delta H^0 = -49.4 \text{ kJ mol}^{-1} \tag{23}$$

The photolysis and photoionization of NO_2, as is well-known in atmospheric research, leads to complex chemistry, including the formation of ozone and both nitrous and nitric acids. There is then more than one possible origin of the NO_3^-. For example, photolysis of NO_2 yields O atoms that can either directly oxidize

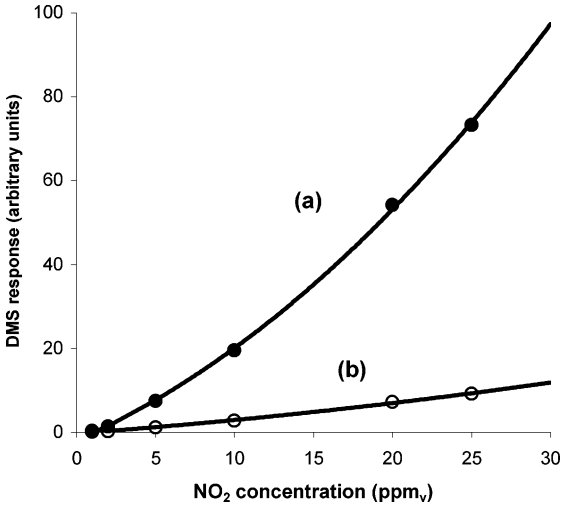

Figure 10. Negative ion DMS signal for NO_2: (a) peak area, $A = 0.0555c^2 + 1.6426c - 1.9066$, $R^2 = 0.9996$; (b) peak height, $H = 0.0042c^2 + 0.2764c - 0.2651$, $R^2 = 0.9983$.

NO_2 to NO_3 (eq 24) or oxidize via the formation of ozone (eqs 25 and 26).

$$NO_2 + O + M \rightarrow NO_3 + M \qquad \Delta H^0 = -205.2 \text{ kJ mol}^{-1} \tag{24}$$

$$O_2 + O \rightarrow O_3 + M \qquad \Delta H^0 = -106.5 \text{ kJ mol}^{-1} \tag{25}$$

$$NO_2 + O_3 \rightarrow NO_3 + O_2 \qquad \Delta H^0 = -98.6 \text{ kJ mol}^{-1} \tag{26}$$

NO_3, having a very high electron affinity (3.91 eV), can then accept an electron from O_2^- or NO_2^- (eqs 27 and 28).

$$O_2^- + NO_3 \rightarrow O_2 + NO_3^- \qquad \Delta H^0 = -335 \text{ kJ mol}^{-1} \tag{27}$$

$$NO_2^- + NO_3 \rightarrow NO_2 + NO_3^- \qquad \Delta H^0 = -158 \text{ kJ mol}^{-1} \tag{28}$$

Another possibility is the exothermic O^- transfer reaction from NO_2^- to NO_2 (eq 29).

$$NO_2^- + NO_2 \rightarrow NO + NO_3^- \qquad \Delta H^0 = -63.1 \text{ kJ mol}^{-1} \tag{29}$$

The formation of the solvating HNO_3 must involve water as a precursor. An intracluster reaction of the hydrated anion $NO_2^-(H_2O)_n$ cannot be invoked, but HNO_3 could be formed by the combination of OH radicals, produced by photolysis of water, with NO_2 (eq 30). This is a well-known reaction in the atmosphere.[43,44]

$$OH + NO_2 \rightarrow HNO_3 \qquad \Delta H^0 = -206.4 \text{ kJ mol}^{-1} \tag{30}$$

The detection limit for NO_2 at a signal-to-noise level of 3:1 is 1 ppm_v. Since this value is obtained by the initial photoionization of a very low concentration of NO_2, it is obvious that the use of a

dopant such as benzene to provide a larger concentration of electrons would lead to a much lower detection limit. Such an experiment has not been performed.

CONCLUSIONS

A DMS operating at atmospheric pressure with a photoionization source can be used for the detection of analytes in low concentrations. The planar design of the spectrometer permits the fast (~1 s) and simultaneous recording of both positive and negative ion spectra, enhancing its analytical identification power. Suitable dopants, used in low concentrations (~2 ppm_v) to initially absorb photons from the UV source, increase the efficiency of analyte ionization and give limits of detection below the ppm level in both positive and negative ion modes.

Photoionization of benzene or higher aromatics as dopants provides both positive molecular ions and low-energy electrons that are rapidly thermalized at atmospheric pressure. Subsequent ion−molecule reactions lead to the ions constituting the observed spectra. Although the benzene cation cannot protonate neutral benzene, it does form protonated DMMP and protonated butanone. Protonated DMMP can be formed by exothermic proton transfer from the benzene cation, but the analogous reaction with butanone is sufficiently endothermic that reaction probably does not occur. The reaction of a benzene cation solvated either by a water molecule or by a butanone molecule is calculated to be sufficiently exothermic for proton transfer to occur. In the presence of a dopant the limits of detection are in the low or sub ppb_v range: DMMP 0.7 ppb_v, butanone 1.7 ppb_v, and similar values, not described in the text, were obtained for 2-pentanone and 3-heptanone. These LODs are of the same order as we have found using ^{63}Ni ionization.

It is somewhat surprising that benzene provides a source of protons in APPI, but it is not surprising that acetone, whose molecular ion can transfer a proton to acetone in an exothermic reaction, is also an excellent source of protons. Both molecules function well under low-humidity conditions, but when the humidity is high, ion hydration leads to the formation of the hydrated proton that can limit the chemical ionization of an analyte. A second problem with a high water content is that although the water molecule is not ionizable with krypton resonance radiation it does absorb photons and then limits total ionization. As for any chemical ionization system, the experimental conditions such as purity of transport gas, ambient water, and analyte concentrations affect the DMS spectrum.

The negative ion DMS spectrum of sulfur hexafluoride and that of nitrogen dioxide contains a single peak. At low concentration the intensity of the peak in the SF_6 spectrum obtained with benzene or acetone as dopant is a linear function of concentration. The LOD is 1×10^2 ppb_v. The intensity of the signal for nondoped NO_2 in the concentration range of 1−30 ppm_v shows a nonlinear dependence on concentration. The mass spectrum at high concentration shows the presence of NO_3^- rather than NO_2^-. The LOD under these conditions is 1×10^3 ppb_v.

This work demonstrates that photoionization is a viable alternative to ^{63}Ni as a source of ions in the DMS. The use of a dopant such as acetone or benzene allows operation in both negative and positive ion modes. As with any ionization technique operating at atmospheric pressure, direct sampling of mixtures without prior chromatographic separation would lead to complex, competitive ion-molecule chemistry.

(43) Sakamaki, F.; Hatakeyama, S.; Akimoto, H. *Int. J. Chem. Kinet.* **1983**, *15*, 1013−29.
(44) D'Ottone, L.; Campuzano-Jost, P.; Bauer, D.; Hynes, A. J. *J. Phys. Chem. A* **2001**, *105*, 10538−43.

ACKNOWLEDGMENT

The authors are very grateful to Muning Zhong, David Wheeler, and Evgeny Krylov for technical support and helpful discussions.

Received for review December 14, 2005. Accepted April 7, 2006.

AC052213I